

Q-estimation from uncorrelated Vibroseis VSP model data

Arnim B. Haase

ABSTRACT

A known method for velocity dispersion estimation and Q-factor calculation from uncorrelated Vibroseis records is investigated. In this method pilot sweeps are partitioned into time segments by successive windowing, each with a different central frequency. These segments are cross-correlated with the entire received sweep at all VSP-stations allowing the automatic picking of frequency and depth dependent travel times and the calculation of velocity dispersion. The method is tested with two synthetic zero-offset VSPs. Q-factors can be recovered fairly accurately away from the near-field in the special case of a homogeneous earth. Velocity dispersion and the Q-factor derived from it are quite sensitive to stratigraphic effects.

INTRODUCTION

In our continuing search for improved Q-estimation algorithms and a better understanding of stratigraphic attenuation effects we took note of a recent paper by Sun et al. (2009) which describes the estimation of velocity dispersion from uncorrelated Vibroseis data. Once velocity dispersion is known Q-factors are computed with the aid of a well known velocity dispersion equation. How does this approach perform in the presence of stratigraphic attenuation? What is the estimation error when Q is recovered from a homogeneous model? To answer these questions, model data are generated with the Weyl/Sommerfeld integral (3D wave field for a 1D earth model) for two situations: Firstly, a synthetic zero-offset VSP is computed for the homogeneous case of constant velocities and constant densities and assuming $Q = 50$. Secondly, the Ross Lake velocity log and density log are used as a model for synthetic zero-offset VSP computations, again assuming $Q = 50$. Velocity dispersion is estimated from the two synthetic zero-offset VSPs, and then $Q(z)$ is computed.

REVIEW OF THE VELOCITY DISPERSION ALGORITHM

Sun et al. (2009) use a *moving window cross-correlation* method to determine frequency and depth dependent travel-times. Then, from travel-time differences, Δt , across a chosen depth interval and the thickness, Δz , of this interval, frequency dependent velocities, $V(f,z)$, are calculated. The method assumes that a pilot sweep is available. This pilot sweep is partitioned into time segments by successive windowing. The windows of choice for this work are Gaussian bells. Sun et al. (2009) specify that these windows must be longer than a few wave lengths. Figure 1 shows the start of a synthetic pilot sweep computed for this study. Sweep length is 20 s, sweep range is 10 Hz to 250 Hz and there is a 400 ms *cos*-taper at either end of the sweep. Also displayed (in red) is the result of multiplication with the first (low-frequency) window. Because this is a synthetic pilot sweep all amplitudes away from the tapered end zones are unity. An increase in frequency with increasing time is also noticeable. The red wavelet in Figure 1 represents a narrow band *wave-package* which is cross-correlated with the entire received sweep at all VSP-stations. Thus the travel-time of this particular *wave-package* to all VSP-stations

can be determined. Because a range of *wave-packages* with different frequency bands is chosen, frequency dependent travel-times can be obtained.

Figure 2 shows the beginning of received sweeps at two different VSP-stations (at $Z = 672$ m and at $Z = 1296$ m depth). Amplitude decay with depth and with frequency can be observed. Also apparent is the delayed onset of the signal at the deeper station. Less noticeable is the increased decay rate at depth. The cross-correlation result of the received sweep at the deepest station with a low-frequency *wave-package* is plotted in Figure 3. The black curve (envelope) in Figure 3 represents instantaneous amplitudes. Travel-times are automatically picked from the envelope maximum location. As expected, these maximum locations are sensitive to the size of the sample interval. When velocities are computed from travel-time differences over a 106 m depth interval, and its thickness, the result is meaningless for a sample interval of $\Delta t = 1$ ms. Matters improve for $\Delta t / 8$ and even more so for $\Delta t / 64$ as can be seen in Figure 4. Even less *numerical jitter* is found when employing double precision arithmetic as demonstrated in Figure 5. $\Delta t / 64$ and double precision are used for all computations below, except for Figure 6, where the results of further Δt – reduction are explored. Note the logarithmic frequency scale for Figures 4 to 6. For Q-estimation purposes straight lines will be fitted to $V(\ln(f))$ and because of that fact some *numerical jitter* is assumed to be tolerable. The variable f in $V(\ln(f))$ is the instantaneous frequency in the centre of the current correlation window.

Q OF THE HOMOGENEOUS MODEL

All frequency dependent velocities obtained thus far are computed for the homogeneous model at a depth of 1243 m. At that depth near-field effects are expected to be negligible. For Q-estimation from velocity dispersion Sun et al. (2009) use the following well known equation which they re-derive:

$$(1) \quad \frac{V(f_2)}{V(f_1)} \approx 1 + \frac{1}{\pi Q} \ln\left(\frac{f_2}{f_1}\right)$$

where $V(f)$ is the frequency dependent velocity.

From Equation 1 the quality factor Q is found to be

$$Q = \frac{\ln\left(\frac{f_2}{f_1}\right)}{\pi\left(\frac{V(f_2)}{V(f_1)} - 1\right)} \quad (2)$$

$V(f_1)$ and $V(f_2)$ are determined from velocity dispersion curves by *least-square-error* straight line fitting to $V(\ln(f))$. For n frequency dependent velocity values the straight line departure is minimized (in the *least-square-error* sense) by setting

$$\frac{d}{da} \left[\sum_{i=1}^n [V(f_i) - a \ln f_i - b]^2 \right] = 0 \quad , \quad (3)$$

giving

$$a = \frac{\sum_{i=1}^n [V(f_i)(\ln f_i)] - b \sum_{i=1}^n [\ln f_i]}{\sum_{i=1}^n [\ln(f_i)]^2} \quad , \quad (4)$$

and by setting

$$\frac{d}{db} \left[\sum_{i=1}^n [V(f_i) - a \ln f_i - b]^2 \right] = 0 \quad , \quad (5)$$

giving, with Equation 4

$$b = \frac{\left(\frac{\sum_{i=1}^n [V(f_i)(\ln f_i)]}{\sum_{i=1}^n [\ln(f_i)]^2} - \frac{\sum_{i=1}^n [V(f_i)]}{\sum_{i=1}^n [\ln(f_i)]} \right)}{\left(\frac{\sum_{i=1}^n [\ln(f_i)]}{\sum_{i=1}^n [\ln(f_i)]^2} - \frac{n}{\sum_{i=1}^n [\ln(f_i)]} \right)} \quad . \quad (6)$$

With

$$V(f_i) = a \ln f_i + b \quad , \quad (7)$$

Equation 2 now becomes

$$Q = \frac{\ln \left(\frac{f_2}{f_1} \right)}{\pi \left(\frac{(a \ln(f_2) + b)}{(a \ln(f_1) + b)} - 1 \right)} \quad . \quad (8)$$

Frequency dependent velocities $V(f)$ for three different depth levels ($Z = 119$ m, $Z = 231$ m and $Z = 456$ m) and straight lines fitted to these curves in the *least-square-error* sense with Equations 4, 6 and 7 are plotted in Figure 7. For $Z = 456$ m (the green curve in Figure 7), and deeper, there is little near-field influence and the straight line fit is a good approximation to $V(\ln(f))$. For $Z = 231$ m (the red curve in Figure 7), and shallower, the near-field dominates, leading to increasing straight line fit errors with decreasing depth Z . A similar near-field response is described in a previous report (Haase and Stewart, 2008). Note the convergence of all three $V(f)$ curves at relatively high frequencies. Figure 8 shows the result of computing $Q(z)$ with Equation 8 for 21 different depth levels. For

comparison purposes the input model parameter of $Q = 50$ is added to the display. Away from the near-field the model Q is recovered quite well in this homogeneous situation.

Q OF THE ROSS LAKE MODEL

How sensitive are frequency dependent velocity estimates to real earth situations where velocities and densities are variable? To answer this question a zero-offset synthetic VSP is computed using velocity and density logs of the Ross Lake survey. Ross Lake velocity and density values are displayed in Figure 9. Note the fill-in values above and below the log. Frequency dependent velocities estimated from this synthetic Ross Lake VSP are shown in Figure 10. Because velocities are increasing with depth the curves in Figure 10 do not converge at the high frequency end of the plot (compare to the homogeneous medium result in Figure 7). $V(f)$ at $Z = 119$ m (the blue curve in Figure 10) is well behaved (except maybe for the remnant near-field effect) because log-velocities and log-densities are constant at that depth level as can be seen in Figure 9. At $Z = 231$ m and 456 m (the red and the green curves in Figure 10) however the effect of stratigraphy on velocity dispersion is apparent. Considering that the upper frequency limit is commonly 60 Hz to 80 Hz it would be difficult to fit reasonable straight lines to $V(\ln(f))$ because of the poor in-band signal to noise ratio. Nonetheless, fitting straight lines to $V(\ln(f))$ at 21 different depth levels and then computing the quality factors with Equation 8 leads to the red $Q(z)$ curve in Figure 11; the curves of Figure 8 are added for comparison purposes. It appears that velocity dispersion $V(f)$ and Q -factors derived from $V(f)$ are quite sensitive to stratigraphic effects because the model Q -factor of 50 cannot be recovered in some depth regions.

CONCLUSIONS

The *moving window cross-correlation* method for velocity dispersion estimation and Q -factor calculation from uncorrelated Vibroseis records suggested by Sun et al. (2009) is investigated. A pilot sweep is chosen and two synthetic zero-offset VSPs are computed. Frequency dependent velocities are calculated from travel-time differences, and these travel-times are computer-picked from instantaneous amplitude maxima. As it turns out, time pick accuracy is a crucial parameter in this procedure. It can be controlled by the size of the sample interval employed, and FFT-domain interpolation is used to this end. Model Q -factor recovery away from the near-field is good for the special case of a homogeneous earth. Velocity dispersion $V(f)$ and Q -factors computed from $V(f)$ appear to be quite sensitive to stratigraphic effects. It remains to be seen whether a suitable stratigraphic compensation can be developed that removes stratigraphic effects from velocity dispersion and thereby reduces Q -estimation errors.

ACKNOWLEDGEMENTS

Support from the CREWES Project at the University of Calgary and its industrial sponsorship is gratefully acknowledged.

REFERENCES

- Haase, A.B., and Stewart, R.R., 2008, Modeling near-field effects in VSP-based Q -estimation: CREWES Research Report, Volume 20
Sun, L.F., Milkereit, B., and Schmitt, D.R., 2009, Measuring velocity dispersion and attenuation in the exploration seismic frequency band: *Geophysics*, **74**, WA113-WA122.

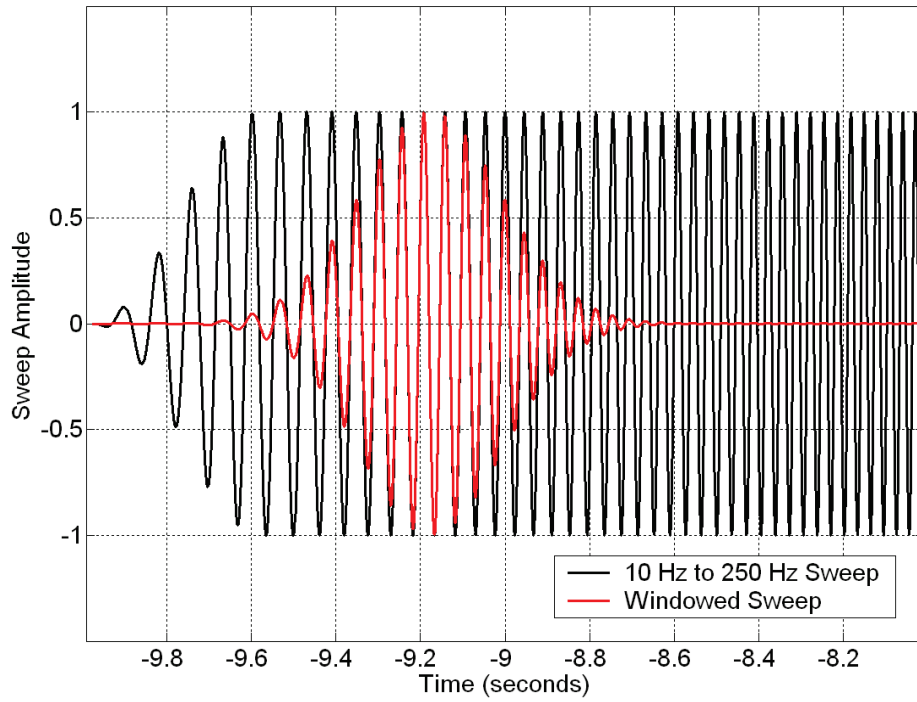


FIG. 1. First part of a synthetic pilot sweep as a function of time.

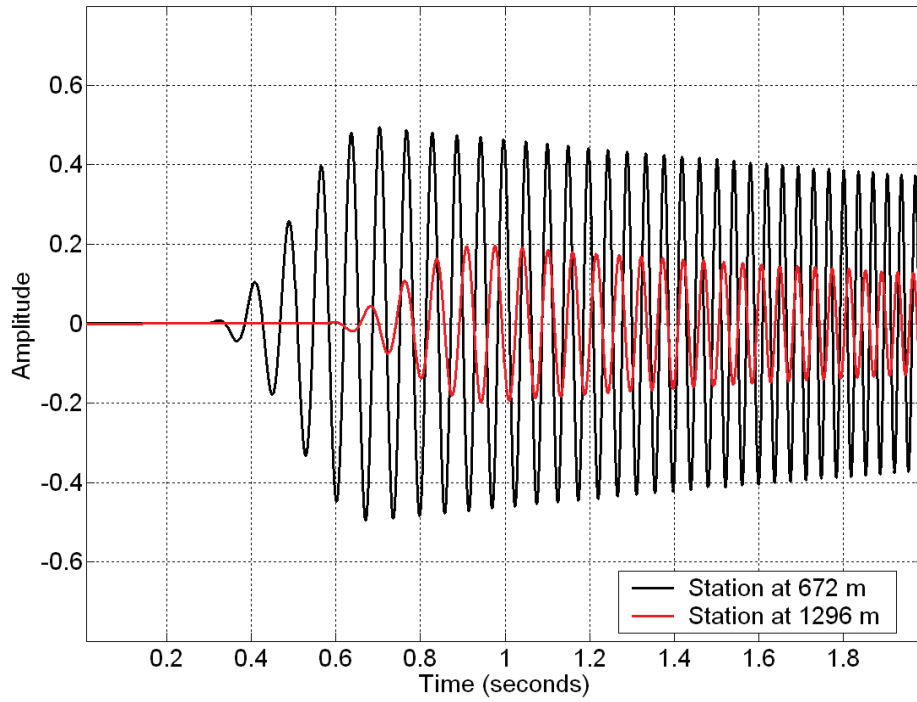


FIG. 2. Uncorrelated VSP-Trace as Function of Time.

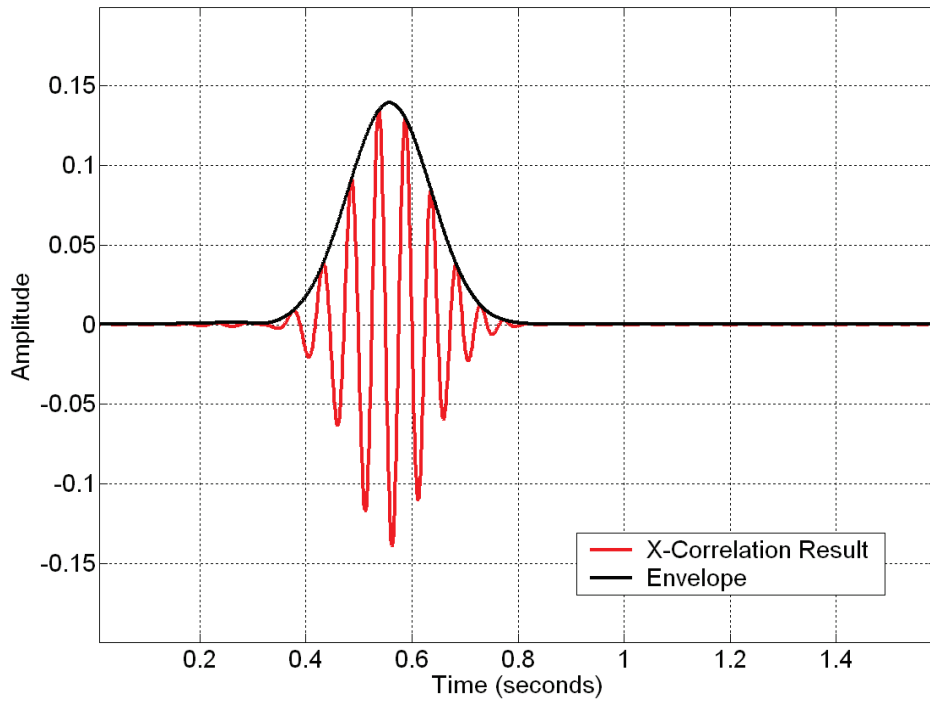


FIG. 3. Cross-Correlation of Windowed Pilot-Sweep and VSP-Trace.

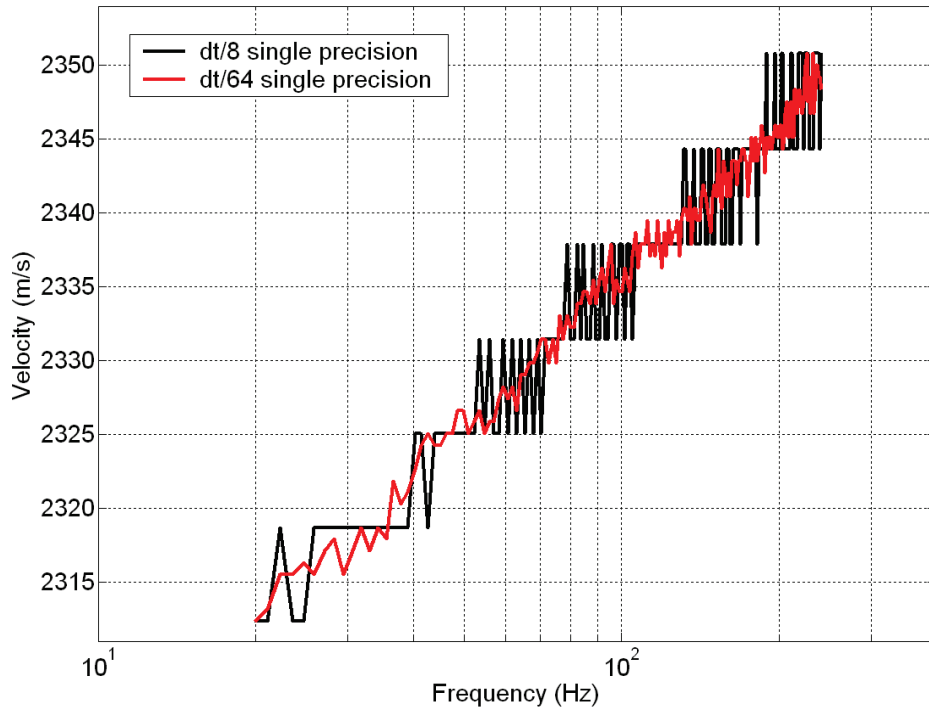


FIG. 4. Velocity as Function of Frequency (sample interval test).

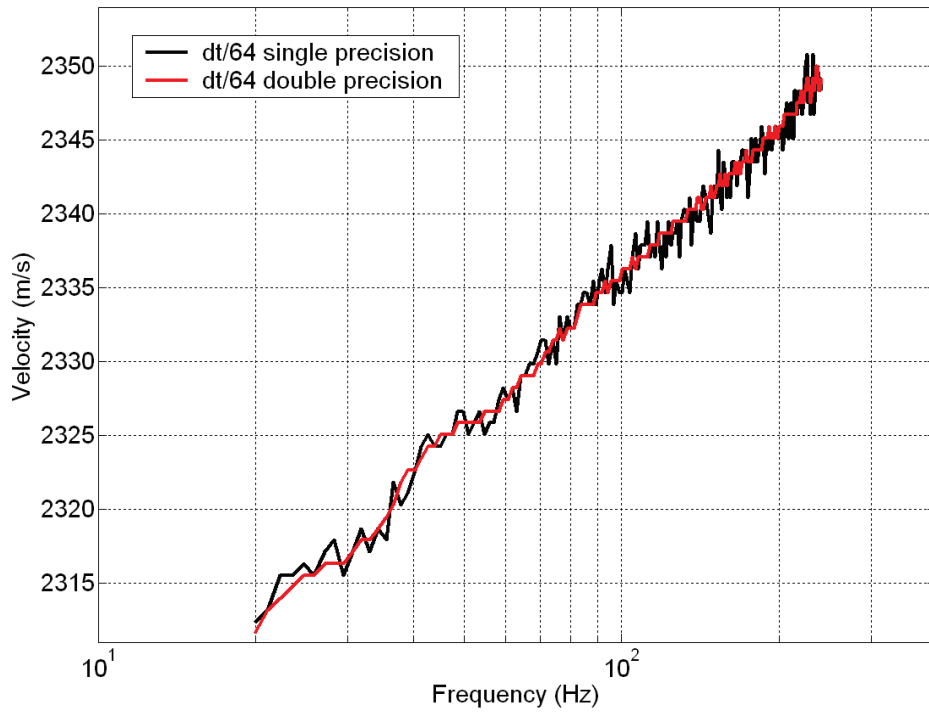


FIG. 5. Velocity as Function of Frequency (single precision versus double precision).

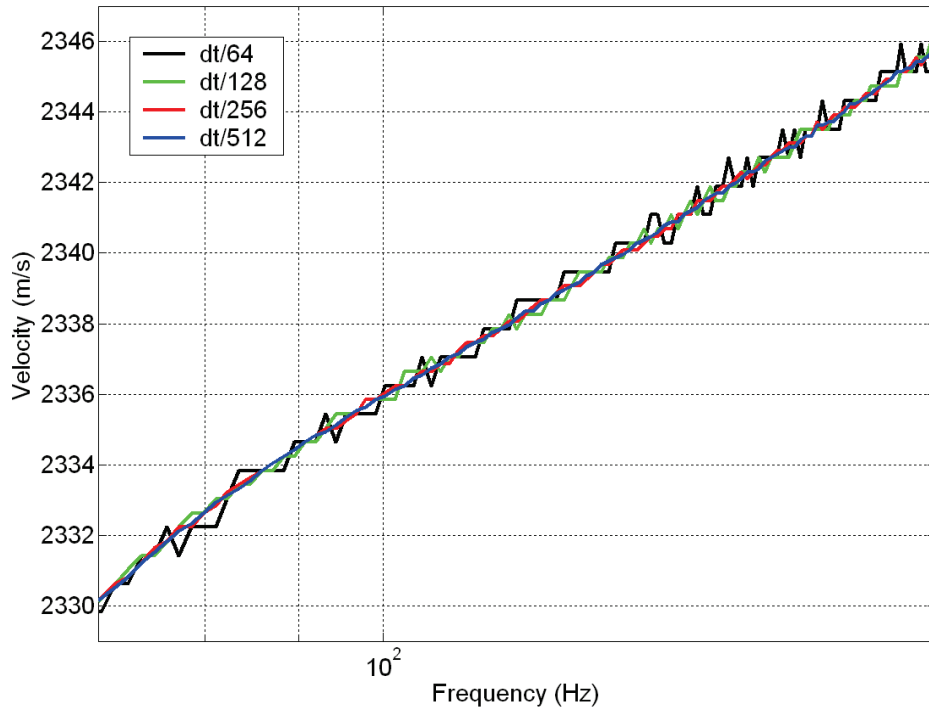


FIG. 6. Velocity as Function of Frequency (sample interval test).

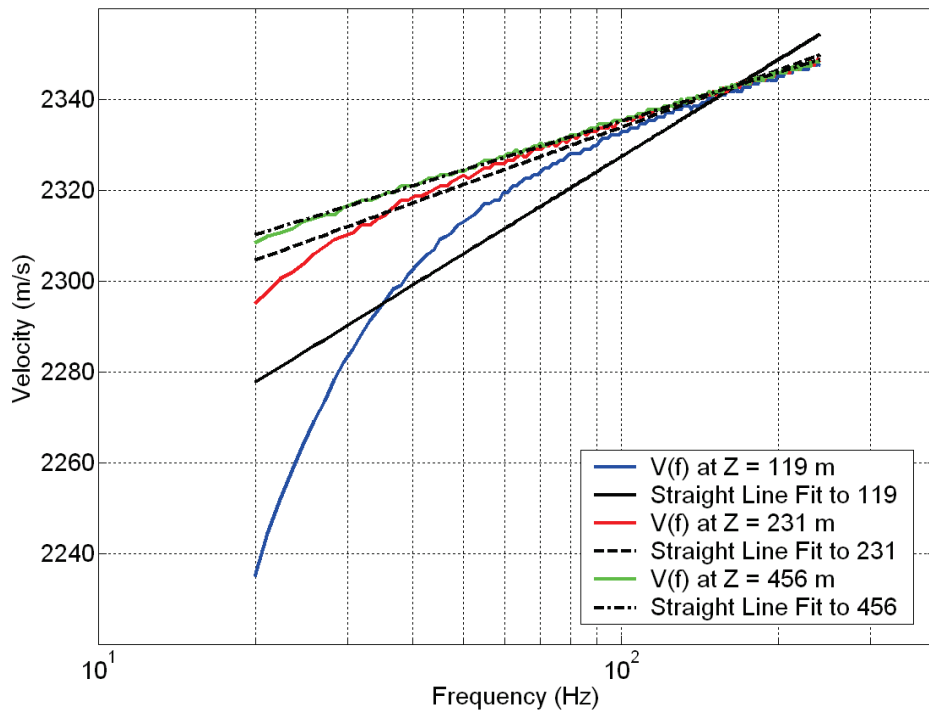


FIG. 7. Frequency Dependent Velocities at Different Depths for Homogeneous Model.

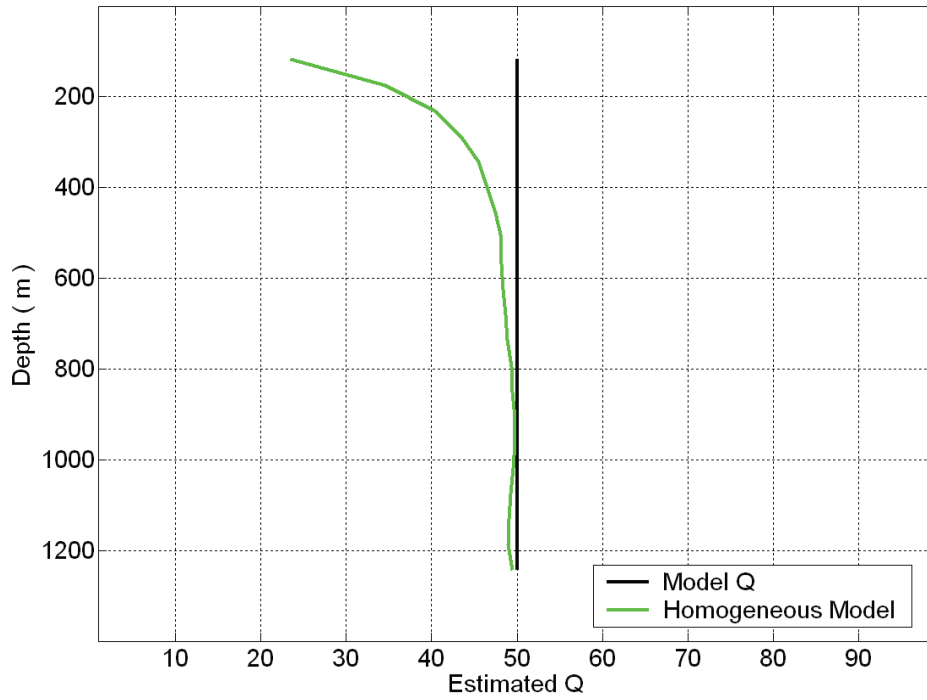


FIG. 8. Q-Estimate by Velocity Dispersion Method (homogeneous model).

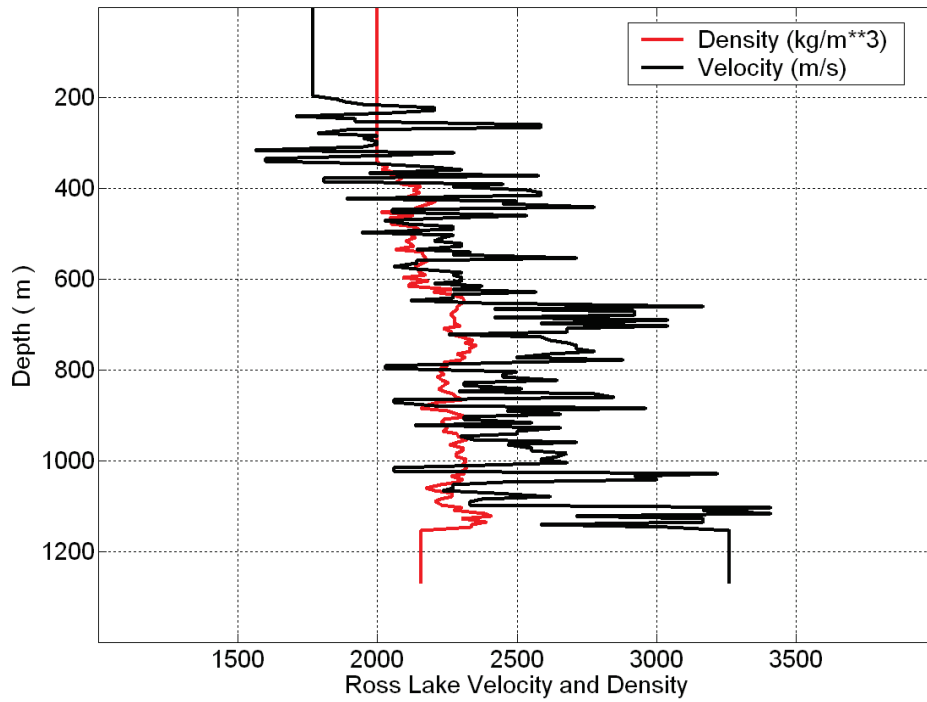


FIG. 9. Velocities and Densities taken from Ross Lake Well-Log.

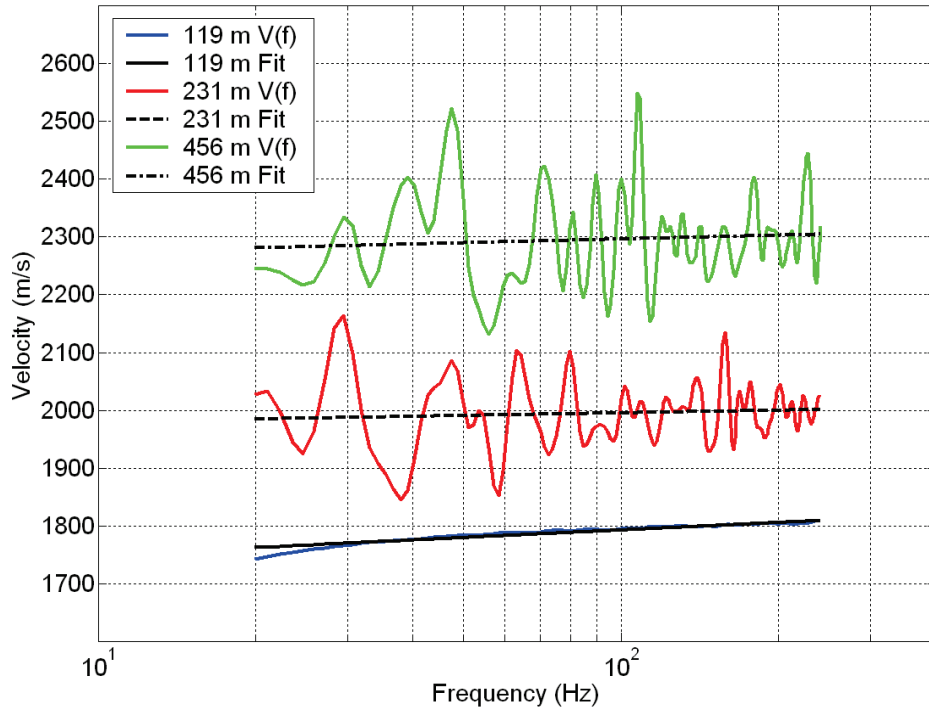


FIG. 10. Frequency Dependent Velocities at Different Depths for Ross Lake Model.

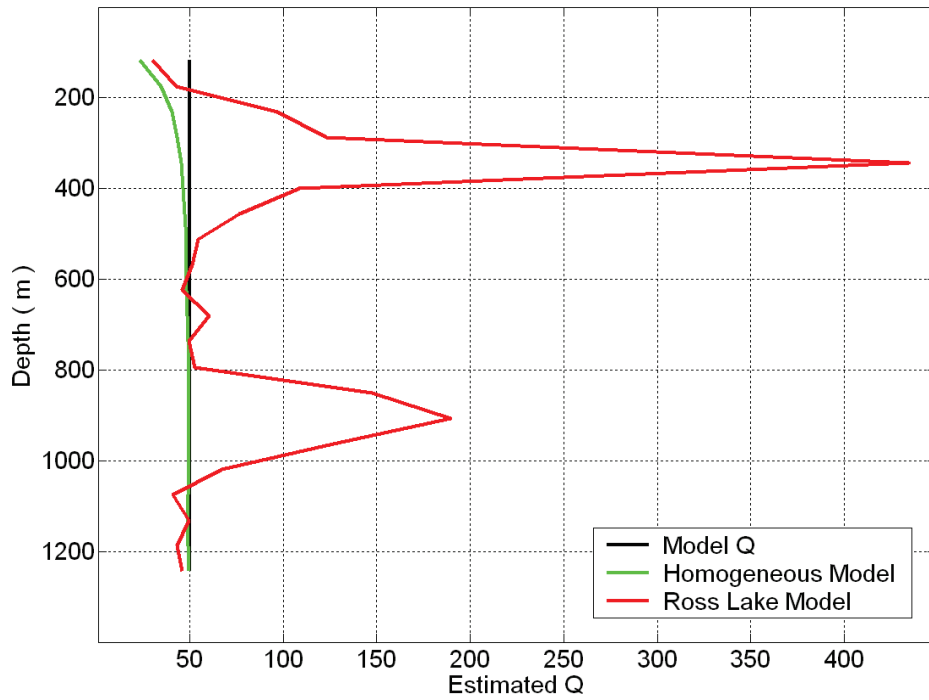


FIG. 11. Q-Estimate by Velocity Dispersion Method (both models).